CARBON 49 (2011) 3544–3552

available at www.sciencedirect.com

ScienceDirect

journal homepage: www.elsevier.com/locate/carbon

Gas sensors based on thick films of semi-conducting single walled carbon nanotubes

Yann Battie [a,*], *Olivier Ducloux* [b], *Philippe Thobois* [b], *Nelly Dorval* [b], *Jean Sébastien Lauret* [c], *Brigitte Attal-Trétout* [b], *Annick Loiseau* [a]

[a] *LEM ONERA-CNRS UMR 104, 29 Av. de la Division Leclerc, 92322 Châtillon, France*
[b] *ONERA – DMPH, 29 Av. de la Division Leclerc, 92322 Châtillon, France*
[c] *LPQM, ENS Cachan CNRS, 94245 Cachan, France*

ARTICLE INFO

Article history:
Received 20 January 2011
Accepted 8 April 2011
Available online 22 April 2011

ABSTRACT

A comparative study was made of sorted semi-conducting single walled carbon nanotube (SWCNT) films and unsorted SWCNT films for gas sensing applications. The transmission line method is used to monitor separately the SWCNTs film resistance and the contact resistance between electrodes and the SWCNTs, thus revealing that the sensing mechanism mainly relies on a modification of the tube conductivity during gas exposure. The fabricated sensors demonstrate a detection limit of 20 ppb NO_2 and 600 ppb NH_3 mainly attributed to experimental setup limitations. Moreover, semi-conducting nanotubes happened to be 2.5 times more sensitive to NH_3 than unsorted ones, thus proving that selectivity can be improved by sorting the SWCNTs. The temperature dependence of the sensor sensitivity was studied, and a good agreement was found between experimental results and the Langmuir adsorption model.

1. Introduction

The one dimensional molecular structure of single walled carbon nanotubes (SWCNTs) consists of a graphene sheet rolled up into a cylinder. The small size, large surface to volume ratio and highly environment-sensitive electrical properties of SWCNTs make them a great candidate for gas sensing applications.

In 2000, Kong et al. [1] showed that the electrical resistance of SWCNTs was modified when exposed to gaseous molecules such as NO_2 or NH_3. Depending on their chirality, SWCNTs can exhibit metallic or semi-conducting properties. In the case of sensor devices based on a single nanotube, it can be a source of irreproducibility. This problem can be overcome using SWCNT networks, as shown by Nanomix Inc. [2]. This type of sensor offers better reproducibility due to the overall averaging of the electrical properties of individual tubes.

Simultaneously, lots of efforts have been put in the development of SWCNT sorting techniques, including dielectrophoresis [3], ion exchange chromatography [4] and density gradient ultracentrifugation (DGU) [5]. This last method enables the separation of metallic carbon nanotubes from semi-conducting ones and is increasingly used to improve reproducibility of SWCNT-based devices [6,7]. In the field of chemical sensors, sorted SWCNTs have been applied to the detection of organic toxic molecules like TNT and DMMP dissolved in water [8]. The authors report intrinsic selectivity of sorted SWCNTs, with no assistance of any functionalization.

Different gas sensing mechanisms have been reported, such as adsorption of gas molecules at the interstitial sites in the SWCNT bundles, direct charge transfer from the gas molecules adsorbed on the SWCNTs and modulation of the Schottky barrier (SB) level at the interface between semi-conducting SWCNTs and metallic electrodes or at the contacts

* *Corresponding author:* Fax: +33 146734155.
E-mail address: yann.battie@onera.fr (Y. Battie).
0008-6223/$ - see front matter
doi:10.1016/j.carbon.2011.04.054

between semi-conducting and metallic SWCNTs [9]. Up to now, few experimental studies have been undertaken in order to investigate the gas detection mechanism.

Zhang et al. [10] deposited a PMMA passivation layer on different parts of their device in order to show that the change of electrical properties during NO_2 exposure was consistent with a modulation of the Schottky barrier (SB) level. On the contrary, Liu et al. [11] argued that when the nanotube film or the contacts were passivated by PMMA, both the SB and the film were playing a role in the gas detection mechanism. The possible diffusion of gas molecules through the passivation layer was evoked to explain these different results. Studies based on ab initio calculations [12,13] reported that the adsorption of gas molecules on the SWCNTs induced a charge transfer between species, consistent with a modification of the SWCNT conductivity and with the charge transfer estimated from experimental results [14]. Moreover, some works based on spectroscopic impendence measurements [9] evidenced a modulation of the Schottky barrier between semiconducting SWCNTs and metallic SWCNTs during the gas exposure which contributes to modify the SWCNTs film resistance.

On the other hand, Bondavalli et al. [15] developed a SWCNTs gas sensor taking advantage of the SB between a SWCNT network and contact electrodes to obtain selectivity by varying the electrode material. Using this approach, the authors claimed the recognition of complex gases, highlighting the importance of the Schottky barrier in the sensing mechanism. The comprehension of the physical interaction between SWCNT based sensors and gas molecules, has not reached a consensus yet and seems to be highly dependent of the device structure.

In this work, we focused on thick SWCNT films for gas sensing applications and tried to identify the involved gas sensing mechanisms. The transmission line method (TLM) [16,17] was used as a non-invasive technique to monitor separately the SWCNT film resistance and the contact resistance between SWCNTs and metallic electrodes. We showed that the adsorption of gas molecules such as NH_3 or NO_2 on the SWCNTs is the main contributor to the gas detection mechanism for our sensors. The kinetics of gas sensing, depending on the temperature, was then described and compared to a simple adsorption/desorption model. We finally compared the sensitivity to NH_3 and NO_2 of sensors based on unsorted SWCNT films and sorted semi-conducting SWCNT ones, showing that selectivity can be achieved by playing on the electronic properties of the SWCNTs.

2. Experimental details

2.1. Sorting of semi-conducting carbon nanotubes

Unsorted purified SWCNTs (P2-SWCNT), produced by the arc discharge technique were purchased from Carbon Solution Inc., California.

Forty milligrams of SWCNTs were first dispersed in a 10 ml solution of distilled water containing 2% w/v of sodium cholate (SC). This dispersion was first sonicated during 1 h, using an ultrasonic tip (240 W), until a homogeneous suspension was obtained and, second, centrifuged during 1 h at 160,000*g* using a SW41 Beckmann Coulter rotor in order to remove the heaviest particles and bundles. The opaque supernatant was then collected to elaborate the sensor based on as-produced unsorted SWCNTs (S1). The same suspension was also used as a basic solution for sorting SWCNTs by density gradient ultracentrifugation.

The sorting of semi-conducting SWCNTs from the as-produced SWCNT suspension was then achieved using the process proposed by Posseckardt et al. [7] and its efficiency determined using the procedure described by Fleurier et al. [18]. Aqueous dilutions of iodixanol, containing 1.4% w/v SC and 0.6% w/v sodium dodecyl sulfate (SDS), were used as density gradient media. Both surfactants (SC and SDS) are known to enhance the mass difference between metallic and semiconducting SWCNTs by non-covalent adsorption. A linear mass density gradient ranging from 1.08 to 1.19 was formed in a centrifuge tube using a linear gradient master device (Biocomp). After formation of the gradient, 1.5 ml of 60% w/v iodixanol was added at the bottom of the centrifugation tube. A 1.8 ml solution of SWCNT supernatant mixed with iodixanol (27.5% w/v) was then injected into the gradient. The top of the tube was then filled with an aqueous solution containing 1.4% w/v of sodium cholate and 0.6% w/v of sodium dodecyl sulfate. This preparation was finally centrifuged for 14 h at 160,000*g*. A pink layer was clearly observed at the top of the density gradient, corresponding to highly concentrated semi-conducting SWCNTs. This layer was collected by using a flat opened needle and used to elaborate the sensor based on semi-conducting SWCNTs (S2).

2.2. Gas sensor fabrication

The TLM platform was fabricated using standard photolithography procedures. The substrate consists of a 400 μm thick undoped silicon wafer covered with a 200 nm thick thermal oxide layer. A double layer of LOR 5A/S 1813 photoresist was then deposited and patterned using standard photolithography processes. A 80 nm thick layer of platinum was finally deposited by sputtering and patterned using the lift-off technique. Platinum was chosen for its chemical inertness and temperature stability. The TLM pattern consists of a series of rectangular electrodes (500 μm × 50 μm) separated by increasing distances (5 μm, 10 μm, 25 μm, 50 μm and 100 μm).

The dispersed SWCNT solutions were filtered through a nitrocellulose membrane. The volume of the solution was adjusted in order to obtain the desired SWCNT film thickness. The film was thoroughly washed with deionized water to remove the surplus of surfactant and finally reported onto the TLM pattern. The nitrocellulose membrane was finally dissolved with acetone.

The electrical properties of SWCNT films exposed to atmospheric environments are significantly influenced by other molecules like oxygen [19] and especially water molecules [20,21]. In addition, organic molecules like iodixanol and surfactant can act as chemisorption sites for gas molecules. This may increase the sensitivity of sensors based on SWCNT networks but it also generates drift of the sensor responses when exposed to gases and during desorption cycles. To overcome this problem, the sensors were first annealed in a furnace at 300 °C in air during 2 h. After thermal treatment, resistances

of both sensor S1 and S2 decreased dramatically due to an improvement of the tube–tube contacts and tube–electrode contacts induced by the pyrolysis of iodixanol and surfactants [22].

2.3. Characterization

Optical absorption spectroscopic measurements were performed using a UV–Visible/NIR Perkin Elmer spectrometer in the wavelength range 320–1200 nm. The E_{22} band amplitude of absorption spectra was normalized to unity. The scanning electron microscopy (SEM) investigations were performed with a field emission gun scanning electron microscope Zeiss Gemini operating at 15 kV. The surface topography of SWCNT films was obtained by a Dimension 3100 Veeco atomic force microscope operating in taping mode. The transmission electron microscopy (TEM) investigations were performed with a Technai CM20 electron microscope operating at 200 kV. SWCNT film resistances were measured by volt-amperometric technique using an automated system composed of a Keithley 705 multichannel scanner and a Keithley 2601 source-meter. The sensitivity S of the sensor was defined as the ratio between resistance variation ΔR of sensor during gas exposure and sensor resistance R_0 before gas exposure.

The TLM analysis was performed by scanning the five electrode pairs separated by increasing inter-electrodes distances d. The voltage applied between each electrodes pair was fixed to 100 mV. The transmission line method (TLM), used to extract the sheet resistance of the film R_{sh} and the average contact resistance R_c between the metallic electrodes and the film, is based on the following expression:

$$R = 2R_c + R_{sh}\frac{d}{W} \quad (1)$$

where W is the electrode width and R the measured resistance between two electrodes.

3. Results and discussion

The normalized UV–visible–IR absorbance spectra of the as-prepared SWCNTs and sorted SC-SWCNT suspensions are shown in Fig. 1. The E_{22} band and the M_{11} band, centered respectively at 1015 nm and 710 nm, are clearly observed on the spectrum of the as-prepared SWCNT suspension. These bands are also present at the same wavelengths in the spectrum of the sorted SWCNT suspension. Since band positions essentially depend on the nanotube diameter, this result suggests that the tube diameter distribution does not change during the sorting procedure. This behavior has been checked by performing a statistical analysis of the tube diameter using TEM according to the procedure described in [18]. As shown in Fig. 2, sorted and unsorted nanotubes display the same diameter distribution.

The average SWCNT diameter determined from TEM images is in the range 1.3–1.4 nm, similar to the one estimated from the position of the E_{22} band in the UV–visible–IR analysis [23]. After subtracting the continuous background of the spectra, the ratio between the amplitudes of the E_{22} and M_{11} bands can be used to estimate the relative concentration of semi-conducting SWCNTs in both suspensions [5]. The

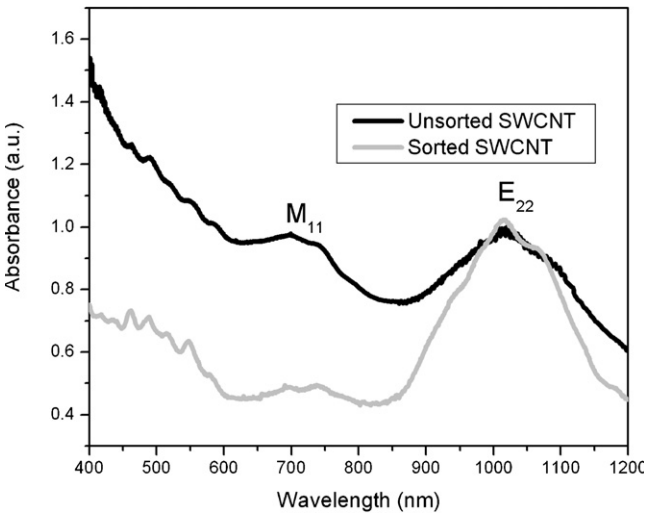

Fig. 1 – Absorption spectra of unsorted and sorted SWCNTs suspensions.

as-prepared suspension and the sorted suspension are respectively composed of 67% and 93% of semi-conducting SWCNTs. Note that the ratio found for unsorted samples is quite consistent with previous estimations, by electron diffraction, indicating a random chirality distribution in this kind of samples [24].

The SEM image of the sensor S2, Fig. 3(a), shows that the SWCNT film covers the TLM platinum electrodes. The AFM topography of the sensor based on sorted SWCNTs (S2) is presented in Fig. 3. It reveals a "spaghetti" like random network composed of agglomerated SWCNT bundles. The average thickness and surface coverage of this network are respectively about 120 nm and 80%. The same characteristics are obtained for S1.

The I–V curves obtained for the five electrode pairs of sensors S1 and S2 are linear in the −2 V to +2 V range (Fig. 4(a)), indicating that ohmic contacts are formed between SWCNTs and metal electrodes. According to previous observations [25,26], the transport properties of our thick SWCNT films can be interpreted using the percolation theory of a random stick network. The linear dependence of the I–V curve can be explained by the high thickness and surface coverage of the "spaghetti like" film which contributes to increase the probability of percolative transport toward the metallic SWCNTs for both sensors and thus to minimize the influence of the SB at the metal electrode/SWCNT film contact on the electrical properties of our sensors [25].

Both metallic and semi-conducting tubes can carry current with a similar resistance, the electronic transport being essentially influenced by the tube-to-tube contact. Indeed, previous studies have demonstrated that electrons are easily transmitted between two semi-conducting or two metallic tubes. However, the junction between semi-conducting and metallic nanotubes induces a SB that can modulate the current flow [27–29]. In accordance with a study conducted by Topinka et al. [30], the resistance of the SWCNT film of S1 sensor, which contains 33% of metallic SWCNTs, is similar to the resistance of the S2 sensor film, which contains 7% of

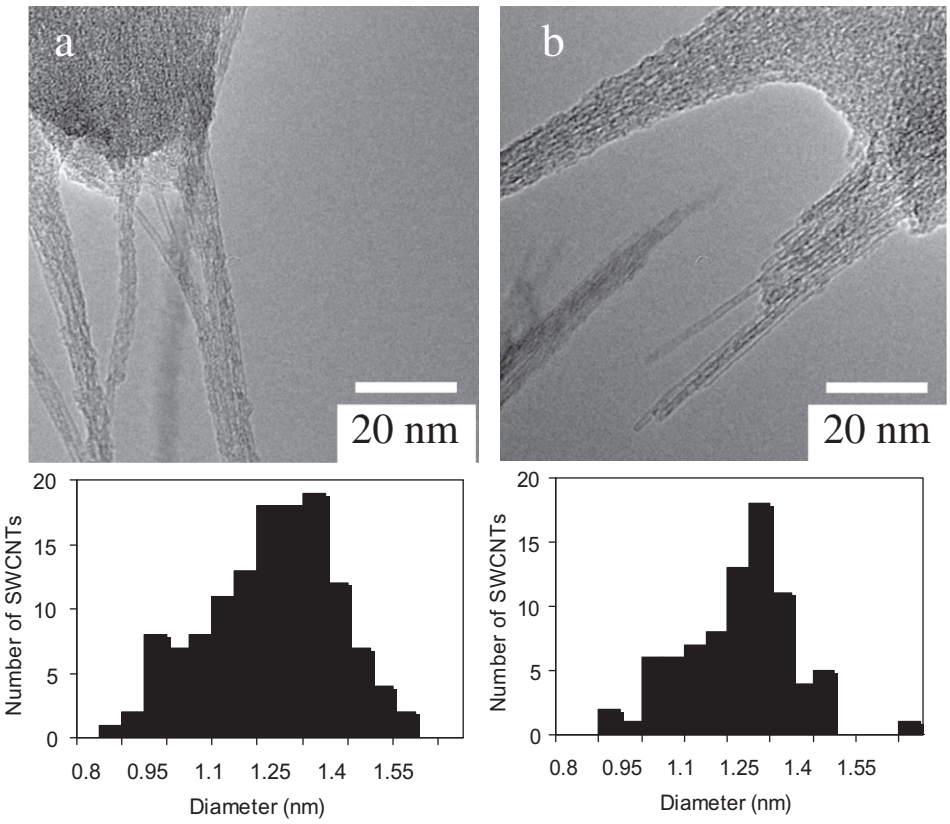

Fig. 2 – TEM pictures and diameter distributions of (a) as-prepared SWCNTs and (b) sorted SWCNTs.

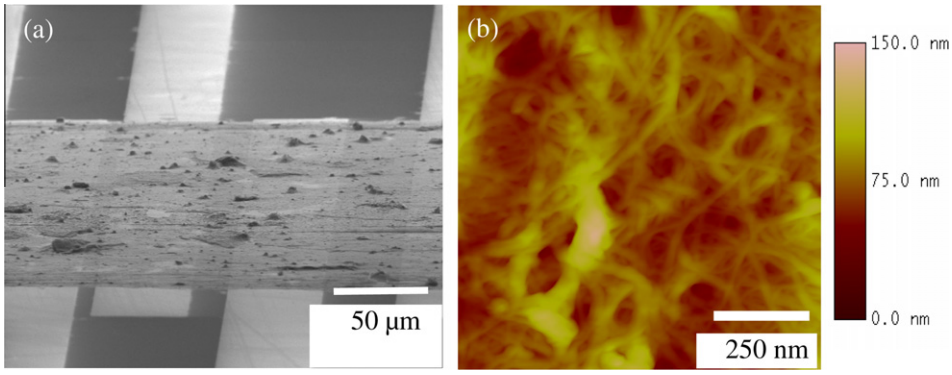

Fig. 3 – (a) SEM image and (b) AFM image of S2 sensor SWCNTs network.

metallic SWCNTs, because the S2 film contains less metallic/semi-conducting SWCNT junctions (Fig. 4).

As shown in Fig. 4(b), a linear relationship between the resistances of S1 and S2 sensors and the inter-electrode spacing only exists for inter-electrode spacings higher than 10 μm. This can be explained by the higher probability to obtain purely metallic SWCNT chains between two electrodes when the inter-electrode distance is small [31]. In agreement with our previous works [22] and other studies proposed by Bondavalli et al. [32], the resistance measured when the inter-electrode spacing is less than 10 μm is mainly attributed to metallic SWCNTs, forming a continuous path similar to a short-circuit between the two electrodes. For that reason, the TLM analysis was realized with data corresponding to the three largest inter-electrode spacings.

Sensors based on SWCNTs were characterized in a test chamber after the stabilization annealing procedure. Each sensor was first heated at 100 °C, during 15 min under vacuum ($2 \cdot 10^{-2}$ mbar), to remove residual water from the test chamber and desorb it from the film. This treatment causes a resistance drop of a few percents, consistent with evaporation of the adsorbed humidity [12,33].

Two pollutant gases were considered: NO_2 and NH_3, dry air being used as a gas carrier. A pressure of 1100 mbar, slightly higher than atmospheric pressure, was maintained during gas exposure in order to prevent water molecules and ambient contaminants from diffusing into the chamber.

Each sensor was exposed to gas during 30 min, then the gas flow was stopped and the sensor was heated during 30 min, at respectively 100 °C in dry air after NH_3 exposure

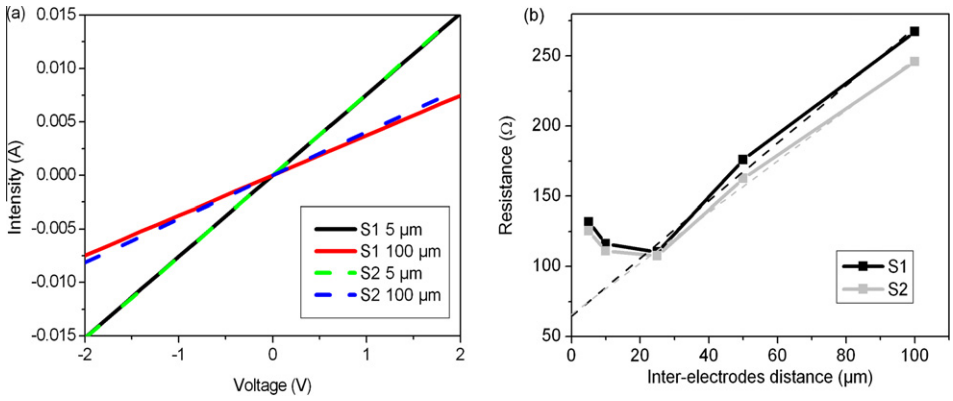

Fig. 4 – (a) *I–V* curves of the S1 and S2 sensors corresponding to 5 μm and 100 μm inter-electrode distances. (b) TLM analysis of S1 and S2 sensors.

and 200 °C in vacuum after NO_2 exposure, in order to recover the initial transport properties of the SWCNT film. The S2 sensor resistance variation during exposure to gases, in the case of an inter-electrode distance equal to 100 μm, is presented in Fig. 5.

Similar time dependence was observed with S1 sensor. Sensors resistances decreased when exposed to NO_2 and an opposite variation was observed during NH_3 exposure, in accordance with other works [1]. The average response time, at room temperature, was comprised in the range 20–30 min. Moreover, the annealing procedure allowed the initial resistance value after gas exposure to be fully recovered. The baseline resistance (i.e. the resistance in dry air atmosphere at 20 °C) was repeatable and stable after several exposure cycles, showing complete desorption of the adsorbed gas molecules.

The measured sensor resolution, at room temperature, increases with the inter-electrode distance. For the higher channel length of S2 (100 μm), the resolution was estimated to 600 ppb for NH_3 and 20 ppb for NO_2. Those levels, currently limited by temperature fluctuations around ambient temperature, are slightly better than those of individual SWCNT sensors and satisfy standards for environmental monitoring applications.

TLM analysis carried out for 0 ppm and 200 ppm of gases (Fig. 6(a) and (b)) showed that the contact resistance between SWCNT films and metallic electrodes (32 Ω) is independent from the gas concentration. This result is in contrast to others studies [32,34] linking the gas sensing mechanism to a modulation of the Schottky barrier existing between metallic electrodes and SWCNTs. This discrepancy can be explained by the high density of SWCNT in our films, which minimizes the SB level and its influence on the sensing mechanism. Only the slope of the curves presented in Fig. 6(a) and (b), i.e. the sheet resistance of the film, is affected by gas exposure. This suggests that gas exposure directly modifies the transport properties of the SWCNT film.

In order to prevent ambient humidity from tampering the measurement results [14], the testing environment was dry and previously dehydrated during gas exposure. According to previous works, based on the measurement of IR spectra of SWCNTs exposed to NH_3 and NO_2 [35] showing that both gas molecules adsorb on SWCNTs, we can unambiguously conclude that the charge transfer induced by NH_3 or NO_2 is the dominant sensing mechanism at stake in our sensors.

The correspondence between gas concentration and S2 sensor sensitivity is reported in the inserts of Fig. 6(a) and (b). In agreement with previous works [35], the S2 sensor exhibits a higher sensitivity to NO_2 than NH_3. This result is consistent with theoretical studies showing that the electronic state density of SWCNTs is dramatically modified by the adsorption of NO_2, but less modified by the adsorption of NH_3 [12]. We can note that the S2 sensor channel with the smaller inter-electrode spacing is relatively insensitive

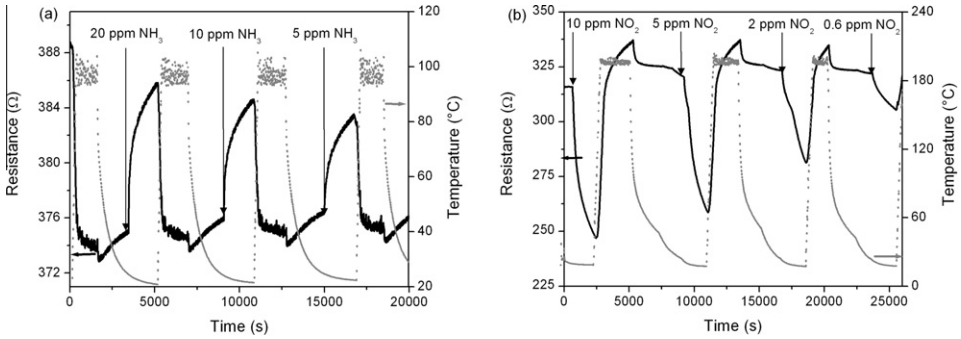

Fig. 5 – Variation of S2 sensor resistance (d = 100 μm) during (a) NH_3 and (b) NO_2 exposures. Temperature variation is shown in grey and dotted lines.

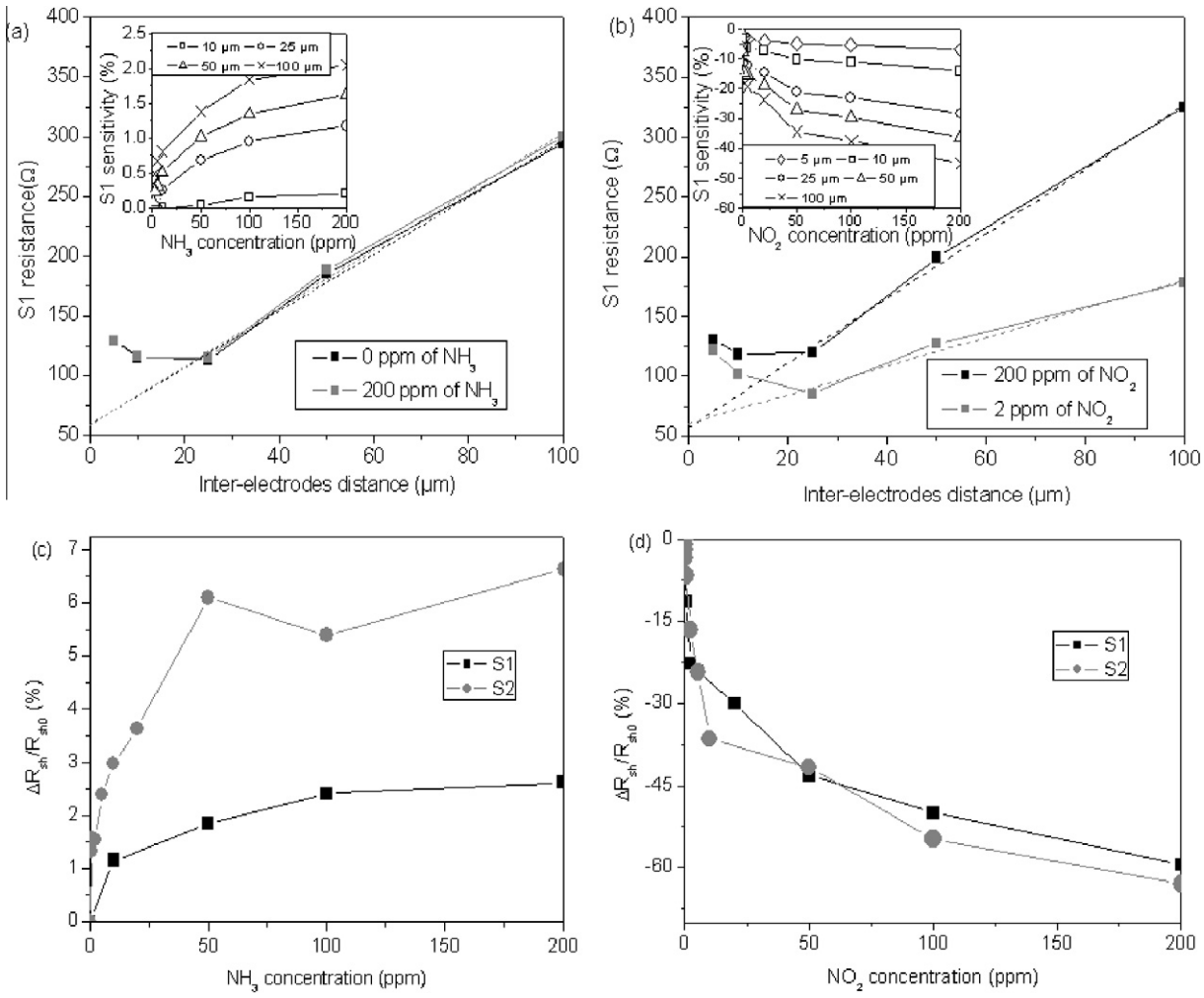

Fig. 6 – TLM analysis of the S2 sensor before and after a 200 ppm (a) NH_3 or (b) NO_2 exposure. In inset: sensibility of the S2 sensor versus (a) NH_3 or (b) NO_2 concentration. Relative variation of the S1 and S2 sheet resistance versus (c) NH_3 and (d) NO_2 concentration.

to NH_3. The charge transfer theoretically calculated is equal to 0.04 electrons per molecule for NH_3 and −0.11 electrons per molecule for NO_2 [13]. In other terms, the adsorption of gas molecules onto SWCNTs is characterized by a higher binding energy and a larger charge transfer with NO_2 than NH_3 [12–14,36].

In the case of NH_3, the curves presented in the inset of Fig. 6(a) are rather linear at low concentrations and tend to saturate at concentration higher than 50 ppm. This saturation, also observed for the smallest inter-electrode spacing during NO_2 exposure (inset of Fig. 6(b)), corresponds to an equilibrium between the adsorption and the desorption of both gases on the SWCNT adsorption sites. This suggests that our sensors can be used for quantitative measurements below 50 ppm.

The absence of Schottky barrier at the metal electrode/SWCNT film contact allows the study of the interaction between the SWCNT film and gas molecules. S1 and S2 sensors show similar sensitivities to NO_2, as shown in Fig. 6(d). However, S2 sensor is 2.5 times more sensitive to NH_3 than S1, as shown in Fig. 6(c), suggesting a better chemical affinity between NH_3 molecules and sorted semi-conducting SWCNTs.

Lemieux et al. demonstrated the possibility of sorting semi-conducting SWCNTs owing to their specific interaction with amine-functionalized surfaces [37]. By analogy, we can assume that NH_3 interacts preferentially with semi-conducting SWCNTs. The chemical nature of NH_3 molecules has to be considered to explain this phenomenon. Zhao et al. [12] have theoretically demonstrated that there is no clear dependence between chirality and NO_2 adsorption on SWCNTs. However, Seo et al. [38] have discussed the selective reactivity of gas on metallic and semi-conducting SWCNTs. According to these studies, the selective adsorption of NH_3 molecules on semi-conducting SWCNTs is related to the electronic state density near the Fermi level. The electron density of semi-conducting nanotubes being lower than these of metallic ones near the Fermi level, the specific adsorption of electron donors like NH_3 on semi-conducting nanotubes is coherent with the reported results [38].

The performances of sensors based on carbon nanotube networks are highly sensitive to temperature. To study the correlation between S1 sensor sensitivity and temperature, the variation of S1 sensor resistance (d = 100 μm) was measured during a 200 ppm NH_3 or NO_2 exposure for different

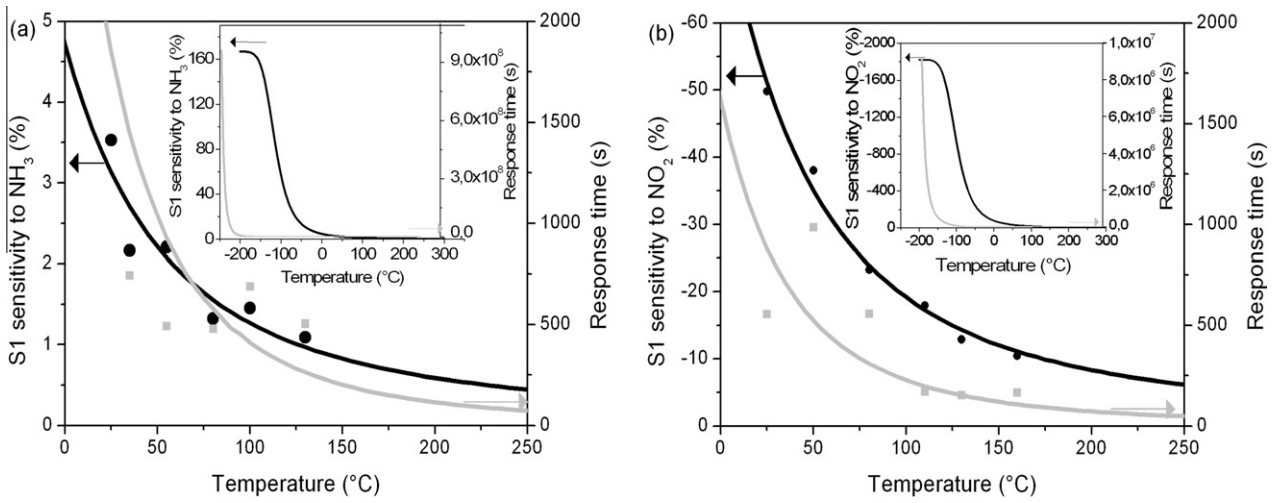

Fig. 7 – S1 sensor sensitivity (in black) and response time (in grey) when exposed to 200 ppm of (a) NH_3 and (b) NO_2. The experimental data are respectively represented by black dots and grey squares, and are compared with the Langmuir model (solid line). In insert, Langmuir modeling from −250 °C to 300 °C.

temperatures. The S1 sensor sensitivity at steady state and the response time were then extracted for each temperature and reported in Fig. 7.

When the temperature increases, S1 sensor sensitivity to NH_3 and NO_2 are highly degraded and the response time decreases. To correlate sensitivity and response time to the temperature, some authors [39–41] proposed to model the sensor response to gas using the Langmuir adsorption model. This model is based on the equilibrium state between adsorption and desorption of gas molecule A on a SWCNT adsorption site θ:

$$A + \theta \leftrightarrow A\theta \tag{2}$$

According to Lee and Strano [41] and assuming that the sensor sensitivity is proportional to the fractional monolayer coverage of molecules adsorbed on the SWCNTs, the sensitivity at the equilibrium S_{st} and the sensor response time τ can be described by the Langmuir isotherm model:

$$S_{st} = \frac{S_0 \cdot Ce^{\frac{-E_a}{kT}}}{1 + Ce^{\frac{-E_a}{kT}}} \quad \text{and} \quad \tau = \frac{\alpha e^{\frac{E_{ad}-E_a}{kT}}}{1 + Ce^{\frac{-E_a}{kT}}} \tag{3}$$

where S_0 is the maximal sensor sensitivity, α a constant, k the Boltzmann constant, C the gas concentration, T the temperature, E_a the binding energy and E_{ad} the activation energy of adsorption.

The best fitting with the experimental data is reported Fig. 7. The Langmuir isotherm model approximates quite well the temperature dependence of the sensor characteristics.

The desorption temperature values calculated from our best fits (inset of Fig. 7) are close to −150 °C for both gases, in the same order of magnitude as experimental infrared measurements estimating these temperatures to −130 °C for NH_3 [42] and near to −80 °C for NO_2 [43].

The binding energy determined from Eq. (3) is equal to −117 meV for NH_3 and −122 meV for NO_2, but the small variation of sensitivity in the experimental temperature range (20–160 °C) leads to a low precision in those evaluations in our case. To compare, the binding energy of NH_3 and NO_2 molecules on single SWCNT or bundles have been respectively estimated by Chang et al. to −180 meV and −420 meV [13]. The negative binding energy is consistent with the decrease of the sensor sensitivity when the temperature increases and corresponds to an exothermic adsorption reaction. The increase of the temperature displaces the equilibrium state towards desorption and consequently decreases the sensitivity because less analytes are immobilized on the nanotube surface, and decreases the response time because the adsorption and desorption reaction kinetics are quicker at higher temperature.

Contrary to some works based on multi-walled carbon nanotubes (MWCNTs) films [9], the small values of binding energy that we have found in both gases are reflecting that the majority of gas molecules are physisorbed on the SWCNTs. This point is consistent with the reversible adsorption of gas molecules on SWCNTs discussed previously.

4. Conclusion

We used the TLM method to discriminate the contact and the sheet resistance of thick SWCNT films. We demonstrated that the high thickness and the high SWCNT density of our films contribute to minimize the influence of SB at the metal electrode/SWCNT contact. The measurement of the sensitivity to NH_3 and NO_2 allowed us to determine the dominant mechanism at stake in gas sensitivity of sensors based on thick and dense SWCNT films. We have demonstrated the decisive advantage of using semi-conducting SWCNTs for improving the sensitivity to NH_3. In the present work, the sensitivity to NH_3 was improved by 2.5 times using sorted semi-conducting SWCNT films, allowing the development of selective sensors based on the SWCNTs chirality. In the future, the selectivity provided by sorted semi-conducting SWCNT films will be evaluated in the case of other common pollutants and warfare agents. Finally, the Langmuir adsorption model was used to describe the temperature dependence of the sensitivity of our sensors to NO_2 and NH_3. The consistency of the experi-

mental measurements with the theoretical model suggests a sensing mechanism based on gas molecules adsorption on the SWCNTs.

Acknowledgments

This work was conducted in the framework of PRF SANAA, a research program granted by ONERA. J.S. Lauret and A. Loiseau acknowledge the National Agency for Research-France (A.N.R., contract: CEDONA (ANR-07-NANO-007-04) for financial support.

REFERENCES

[1] Kong J, Franklin NR, Zhou C, Chapline MG, Peng S, Cho K, et al. Nanotubes molecular wires as chemical sensors. Science 2000;287(5453):622–5.
[2] Star A, Bradley K, Collins PG, Gabriel J-CP, Grune G. Sensitivity control for nanotube sensors. US Patent 0169798, 2005.
[3] Krupke R, Hennrich F, Löhneysen HV, Kappes MM. Separation of metallic from semiconducting single-walled carbon nanotubes. Science 2003;301(5631):344–7.
[4] Zheng M, Jagota A, Semke ED, Diner BA, Mclean RS, Lustig SR, et al. DNA-assisted dispersion and separation of carbon nanotubes. Nat Mater 2003;2(5):338–42.
[5] Arnold MS, Green AA, Hulvat JF, Stupp SI, Hersam MC. Sorting carbon nanotubes by electronic structure using density differentiation. Nat Nanotechnol 2006;1(1):60–5.
[6] Engel M, Small JP, Steiner M, Freitag M, Green AA, Hersam MC, et al. Thin film nanotube transistors based on self-assembled, aligned, semiconducting carbon nanotube arrays. ACS Nano 2008;2(12):2445–52.
[7] Posseckardt J, Battie Y, Fleurier R, Lauret J-S, Loiseau A, Jost O, et al. Improved sorting of carbon nanotubes according to electronic type by density gradient ultracentrifugation. Phys Status Solidi B 2010;247(11–12):2687–90.
[8] Roberts ME, LeMieux MC, Bao Z. Sorted and aligned single-walled carbon nanotube networks for transistor-based aqueous chemical sensors. ACS Nano 2009;3(10):3287–93.
[9] Varghese OK, Kirchambre PD, Gong D, Ong KG, Dickey EC, Grimes CA. Gas sensing characteristics of multi-wall carbon nanotubes. Sensor Actuator B 2001;81(1):32–3.
[10] Zhang J, Boyd A, Tselev A, Paranjape M, Barbara P. Mechanism of NO_2 detection in carbon nanotube field effect transistor chemical sensors. Appl Phys Lett 2006;88(12):123112-1–3.
[11] Liu XL, Luo ZC, Han S, Tang T, Zhang DH, Zhou CW. Band engineering of carbon nanotube field effect transistors via selected area chemical gating. Appl Phys Lett 2005;86(24):243501-1–3.
[12] Zhao J, Buldum A, Han J, Lu JP. Gas molecule adsorption in carbon nanotubes and nanotube bundles. Nanotechnology 2002;13(2):195–200.
[13] Chang H, Lee JD, Lee SM, Lee YH. Adsorption of NH_3 and NO_2 molecules on carbon nanotubes. Appl Phys Lett 2001;79(23):3863–5.
[14] Bradley K, Gabriel J-C P, Briman M, Star A, Grüner G. Charge transfer from ammonia physisorbed on nanotubes. Phys Rev Lett 2003;91(21):219301-1–4.
[15] Bondavalli P, Legagneux P, Pribat D. Carbon nanotubes based transistors as gas sensors: state of the art and critical review. Sensor Actuator B 2009;140(1):304–18.
[16] Jackson R, Graham S. Specific contact resistance at metal/carbon nanotube interfaces. Appl Phys Lett 2009;94(1):012109-1–3.
[17] Koechlin C, Maine S, Haidar R, Trétout B, Loiseau A, Pelouard J-L. Electrical characterization of devices based on carbon nanotube films. Appl Phys Lett 2010;96(10):103501-1–3.
[18] Fleurier R, Lauret JS, Lopez U, Loiseau A. Transmission electron microscopy and UV–vis–IR spectroscopy analysis of diameter sorting of carbon nanotubes by gradient density ultracentrifugation. Adv Funct Mater 2009;19(14):2219–23.
[19] Collins PG, Bradley K, Ishigami M, Zettl A. Extreme Oxygen Sensitivity of Electronic Properties of Carbon Nanotubes. Science 2000;287(5459):1801–4.
[20] Na PS, Kim H, So H-M, Kong K-J, Chang H, Ryu BH, et al. Investigation of the humidity effect on the electrical properties of single-walled carbon nanotube transistors. Appl Phys Lett 2005;87(9):093101–3.
[21] Aguirre CM, Levesque PL, Paillet M, Lapointe F, St-Antoine BC, Desjardins P, et al. The Role of the oxygen/water redox couple in suppressing electron conduction in field-effect transistors. Adv Mater 2009;21(30):3087–91.
[22] Battie Y, Ducloux O, Thobois P, Coffinier Y, Loiseau A. Evaluation of sorted semi-conducting carbon nanotube films for gas sensing application. CRAS 2010;11(5–6):397–404.
[23] Bachilo SM, Strano MS, Kittrell C, Hauge RH, Smalley RE, Weismann RB. Structure-assigned optical spectra of single-walled carbon nanotubes. Science 2002;298(5602):2361–6.
[24] Henrard L, Loiseau A, Journet C, Bernier P. Study of the symmetry of single-wall nanotubes by electron diffraction. Eur Phys J B 2000;13(4):661–9.
[25] Skákalová V, Kaiser AB, Woo Y-S, Roth S. Electronic transport in carbon nanotubes: from individual nanotubes to thin and thick networks. Phys Rev B 2006;74(8):085403-1–085403-10.
[26] Sangwan VK, Behnam A, Ballarotto VW, Fuher MS, Ural A, Williams ED. Optimizing transistor performance of percolating carbon nanotube networks. Appl Phys Lett 2010;97(4):043111-1–3.
[27] Fuhrer MS, Nygrd J, Shih L, Forero M, Yoon Y-G, Mazzoni MSC, et al. Crossed nanotube junctions. Science 2000;288(5465):494–7.
[28] Bachtold A, Fuhrer MS, Plyasunov S, Forero M, Anderson EH, Zettl A, et al. Scanned probe microscopy of electronic transport in carbon nanotubes. Phys Rev Lett 2000;84(26):6082–5.
[29] Purewal MS, Hong BH, Ravi A, Chandra B, Hone J, Kim P. Scaling of resistance and electron mean free path of single-walled carbon nanotubes. Phys Rev Lett 2007;98(18):186808-1–4.
[30] Topinka MA, Rowell MW, Goldhaber-Gordon D, McGehee MD, Hecht DS, Gruner G. Charge transport in interpenetrating networks of semiconducting and metallic carbon nanotubes. Nano Lett 2009;9:1866–71.
[31] Stadermann M, Papadakis SJ, Falvo MR, Novak J, Snow E, Fu Q, et al. Nanoscale study of conduction through carbon nanotube networks. Phys Rev B 2004;69(20):201402-1–3.
[32] Bondavalli P, Legagneux P, Pribat D, Balan A, Nazeer S. Gas fingerprinting using carbon nanotubes transistor arrays. J Exp Nanosci 2008;3(4):347–56.
[33] Tsai JTH, Lu C-C, Li JG. Fabrication of humidity sensors by multi-walled carbon nanotubes. J Exp Nanosci 2010;5(4):302–9.
[34] Peng N, Zhang Q, Chow CL, Tan OK, Marzari N. Sensing mechanisms for carbon nanotube based NH_3 gas detection. Nano Lett 2009;9(4):1626–30.
[35] Ellison MD, Crotty MJ, Koh D, Spray RL, Kaitlin ET. Adsorption of NH_3 and NO_2 on single-walled carbon nanotubes. J Phys Chem B 2004;108(23):7938–43.

[36] Bauschlicher CW, Ricca A. Binding of NH_3 to graphite and to a (9,0) carbon nanotube. Phys Rev B 2004;70(11):115409-1–6.
[37] Lemieux MC, Roberts M, Barman S, Jin YW, Kim JM, Bao Z. Self sorted, aligned nanotube networks for thin-film transistors. Science 2008;321(5885):101–3.
[38] Seo K, Park KA, Kim C, Han S, Kim B, Lee YH. Chirality- and diameter-dependent reactivity of NO_2 on carbon nanotube walls. J Am Chem Soc 2005;127(45):15724–9.
[39] Wongwiriyapan W, Honda S-I, Konishi H, Mizuta T, Ikuno T, Ito T, et al. Single-walled carbon nanotube thin-film sensor for ultrasensitive gas detection. Jpn J Appl Phys 2005;44(2):482–4.
[40] Robinson JA, Snow ES, Badescu SC, Reinecke TL, Perkins FK. Role of defects in single-walled carbon nanotube chemical sensors. Nano Lett 2006;6(8):1747–51.
[41] Lee CY, Strano MS. Understanding the dynamics of signal transduction for adsorption of gases and vapors on carbon nanotube sensors. Langmuir 2005;21(11):5192–6.
[42] Feng X, Irle S, Witek H, Morokuma K, Vidic R, Borguet E. Sensitivity of ammonia interaction with single-walled carbon nanotube bundles to the presence of defect sites and functionalities. J Am Chem Soc 2005;127(30):10533–8.
[43] Larciprete R, Petaccia L, Lizzit S, Goldoni A. The role of metal contact in the sensitivity of single-walled carbon nanotubes to NO_2. J Phys Chem C 2007;111(33):12169–74.